QSAR Studies on the Inhibitory Activity of New Methoxyacrylate Analogues against *Magnaporthe grisea* (Rice Blast Disease)

Young-Seob Song,[†,‡] Nack-Do Sung,[‡] Yong Man Yu,[§] and Bum Tae Kim[†,*]

[†]*Korea Research Institute of Chemical Technology, Daejeon 305-600, Korea*
[‡]*Department of Applied Biology & Chemistry, Chung-Nam National University, Daejeon 305-764, Korea*
[§]*Department of Agricultural Biology, College of Agricultural & Life Science, Chung-Nam National University, Daejeon 305-764, Korea*
Received June 7, 2004

We investigate a series of synthesized β-methoxyacrylate analogues for their 3D QSAR & HQSAR against *Magnaporthe grisea* (Rice Blast Disease). We perform the three-dimensional Quantitative Structure-Activity Relationship (3D-QSAR) studies, using the comparative molecular field analysis (CoMFA) and comparative molecular similarity indices analysis (CoMSIA) procedure. In addition, we carry out a two-dimensional Quantitative Structure-Activity Relationship (2D-QSAR) study, using the Hologram QSAR (HQSAR). We perform these studies, using 53 compounds as a training set and 10 compounds as a test set. The predictive QSAR models have conventional r^2 values of 0.955 at CoMFA, 0.917 at CoMSIA, and 0.910 at HQSAR respectively; similarly, we obtain cross-validated coefficient q^2 values of 0.822 at CoMFA, 0.763 at CoMSIA, and 0.816 at HQSAR, respectively. From these studies, the CoMFA model performs better than the CoMSIA model.

Key Words : QSAR, β-Methoxyacrylates, Strobilurin fungicide, Fluoroolefin

Introduction

Recently, β-methoxyacrylates (**MOA**) have been introduced as several promising fungicides, including azoxystrobin (**AMISTAR**)[1] as a new class of fungicide with a broad spectrum and new mode of action. The β-methoxyacrylate are known to be an inhibitor of the respiratory electron transport (RET) system in mitochondria[2] and to be developed from structural modification of strobilurin[3] oudemansin[4] and myxothiazole,[5] naturally occurring anti-fungal compounds. The β-methoxyacrylate fungicides are used in agriculture and have been subjected to aggressive structural modification for investigation of more suitable fungicides. The structure-activity relationship on toxophore and substituents of β-methoxyacrylate has been validated as an efficacious tool to estimate fungicidal activity and to improve synthetic efficiency for reducing synthetic expenses. To search and develop the β-methoxyacrylate family fungicide, a series of new 70 β-methoxyacrylate analogues with fluorostyrene moiety was synthesized from the reaction of benzyl bromide substituted methoxyacrylates (or methoxyiminoacetates/methoxyiminoacetamides) group at ortho position with oximes having fluorostyrene moiety. The evaluation of fungicidal activities of new 70 β-methoxyacrylate analogues was accomplished in cell-based assay on *Magnaporthe grisea* (Rice Blast Disease), and we obtained a pI_{50} value for each compound. Generally, the 3D-QSAR study has become an efficient tool for the analysis of an effective pharmacophore model and the design of more active compounds even though nothing as yet is known about specific targets. For this purpose, the use of molecular fields as descriptors for the correlation of biological activities with 3D structures has become an efficient tool frequently applied.

In the present paper, we carried out two different quantitative structure-activity relationship (QSAR) methods on 63 β-methoxyacrylate analogues. One is two 3D-QSAR processes, comparative molecular field analysis (CoMFA)[6,7] and comparative molecular similarity indices analysis (CoMSIA).[8] The other is a 2D-QSAR process, HQSAR.[9] In addition, we compared two different approaches in terms of potential for predictability by elucidation of physical properties, the steric, the electrostatic, the hydrophobic and the hydrogen bonding of these molecules and their influence on the fungicidal activity.

Experimental and Computational Methods

Reagent and appliances. All starting materials and reagents were commercially available and used without further purification except as indicated. THF, dichloromethane (DCM), and toluene were dried. Silica gel plates (Merck F254) and silica gel 60 (Merck; 70-230 mesh) were used for analytical and column chromatography, respectively.

^{1}H-NMR and mass spectrometer (Shimadzu C/MS-QP1000) were used to confirm the structure of the prepared substrates. The ^{1}H-NMR spectra were obtained with a Varian Gemini 200 instrument at 200 MHz. The chemical shifts are reported in δ (ppm) and are relative to the central peak of the tetramethylsilane (TMS).

*Corresponding Author. Tel.: +82-42-860-7023; Fax: +82-42-861-0307; e-mail: btkim@krict.re.kr

Synthesis of analogues. The benzyl bromide substituted methoxyacrylate was prepared from subsequence reaction, such as the esterification, formylation, methylation, and bromination of *o*-tolylacetic acid. The benzyl bromide substituted methoxyiminoacetate was synthesized from the sequential reaction of Grignard reaction, oxalation, condensation, and bromination of *o*-bromotoluene according to a conventional method.[10,11] And the benzyl bromide substituted methoxyiminoacetamide was easily obtained by amidation of methoxyiminoacetate with methylamine. Finally, the methoxyacrylate analogues were synthesized from the reaction of phenyloximes substituted fluorovinyl moiety with three types of benzyl bromides.[12,13]

Biological activity. The fungicidal activities of the data set of 70 molecules with their structure are shown in Table 1. The inhibitory value was calculated by comparing the disease area of treatment with the disease area of untreated control and expressed to EC_{50}, the molar concentration for 50% inhibition against *Magnaporthe grisea* (Rice Blast Disease). The pI_{50} value calculated from EC_{50} (μg/ml.), according to the Eq. (1):

$$pI_{50} = -\log(EC_{50} / M.W.) \quad (1)$$

Computational methods. All molecular modeling and statistical analyses were performed using SYBYL 6.9 molecular modeling software (Tripos Inc.).[14] All Structures of the β-methoxyacrylate analogues were obtained through energy minimization with the Tripos force field, and partial atomic charges were added using the Gasteiger-Huckel

Table 1. Methoxyacrylate analogues and their observed fungicidal activities (pI_{50}) against *Magnaporthe grisea* (Rice Blast Disease)

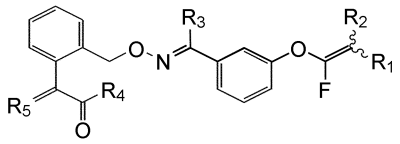

Entry	R_1	R_2	R_3	R_4	R_5	pI_{50}
1[c]	4-CH_3-C_6H_4	H	H_3C	H_3CO	H_3CO-N	7.98
2	3,4-$(CH_3)_2$-C_6H_3	H	H_3C	H_3CO	H_3CO-N	8.72
3	3,5-$(CH_3)_2$-C_6H_3	H	H_3C	H_3CO	H_3CO-N	8.95
4[c]	4-$CH_3(CH_2)_3$-C_6H_4	H	H_3C	H_3CO	H_3CO-N	8.03
5	3-CH_3O-C_6H_4	H	H_3C	H_3CO	H_3CO-N	7.99
6	4-CH_3O-C_6H_4	H	H_3C	H_3CO	H_3CO-N	8.27
7	4-CH_3CH_2O-C_6H_4	H	H_3C	H_3CO	H_3CO-N	8.16
8[c]	4-F-C_6H_4	H	H_3C	H_3CO	H_3CO-N	8.43
9	3-Cl-C_6H_4	H	H_3C	H_3CO	H_3CO-N	8.60
10	4-Cl-C_6H_4	H	H_3C	H_3CO	H_3CO-N	8.16
11	C_6H_5	H	H_3C	H_3CHN	H_3CO-N	9.25
12	3-CH_3-C_6H_4	H	H_3C	H_3CHN	H_3CO-N	9.98
13[a]	4-CH_3CH_2-C_6H_4	H	H_3C	H_3CHN	H_3CO-N	9.89
14	4-CH_3CH_2O-C_6H_4	H	H_3C	H_3CHN	H_3CO-N	8.65
15[b]	4-F-C_6H_4	H	H_3C	H_3CHN	H_3CO-N	10.70
16	C_6H_5	F_3C	H_3C	H_3CO	H_3CO-N	8.96
17	3-CH_3-C_6H_4	F_3C	H_3C	H_3CO	H_3CO-N	8.88
18[b]	4-CH_3-C_6H_4	F_3C	H_3C	H_3CO	H_3CO-N	8.94
19	3,5-$(CH_3)_2$-C_6H_3	F_3C	H_3C	H_3CO	H_3CO-N	9.06
20	3,4-$(CH_3)_2$-C_6H_3	F_3C	H_3C	H_3CO	H_3CO-N	8.71
21[c]	4-CF_3-C_6H_4	F_3C	H_3C	H_3CO	H_3CO-N	8.11
22	4-$CH_3(CH_2)_3$-C_6H_4	F_3C	H_3C	H_3CO	H_3CO-N	8.08
23	3-CH_3O-C_6H_4	F_3C	H_3C	H_3CO	H_3CO-N	9.08
24	4-CH_3O-C_6H_4	F_3C	H_3C	H_3CO	H_3CO-N	8.59
25	4-F-C_6H_4	F_3C	H_3C	H_3CO	H_3CO-N	9.27
26	4-Cl-C_6H_4	F_3C	H_3C	H_3CO	H_3CO-N	9.17
27	3,4-OCH_2O-C_6H_3	F_3C	H_3C	H_3CO	H_3CO-N	8.93
28[b]	3,5-Cl_2-C_6H_3	F_3C	H_3C	H_3CO	H_3CO-N	9.18
29	3-CF_3-C_6H_4	F_3C	H_3C	H_3CO	H_3CO-N	9.01
30	C_6H_5	F_3C	H_3C	H_3CHN	H_3CO-N	9.79
31	4-CH_3-C_6H_4	F_3C	H_3C	H_3CHN	H_3CO-N	8.92
32[c]	4-CH_3CH_2-C_6H_4	F_3C	H_3C	H_3CHN	H_3CO-N	9.05
33	4-F-C_6H_4	F_3C	H_3C	H_3CHN	H_3CO-N	10.24
34[c]	3-Cl-C_6H_4	F_3C	H_3C	H_3CHN	H_3CO-N	9.52
35	C_6H_5	F_3C	F_3C	H_3CO	H_3CO-N	7.50
36	3-CH_3-C_6H_4	F_3C	F_3C	H_3CO	H_3CO-N	7.69
37[b]	4-Cl-C_6H_4	F_3C	F_3C	H_3CO	H_3CO-N	8.06
38	C_6H_5	H	H_3C	H_3CO	H_3CO-HC	9.07
39	3-CH_3-C_6H_4	H	H_3C	H_3CO	H_3CO-HC	9.43
40	4-CH_3-C_6H_4	H	H_3C	H_3CO	H_3CO-HC	8.74
41	3,4-CH_3-C_6H_3	H	H_3C	H_3CO	H_3CO-HC	9.02
42[a]	3-Cl-C_6H_4	H	H_3C	H_3CO	H_3CO-HC	6.86
43	4-CH_3CH_2-C_6H_4	H	H_3C	H_3CO	H_3CO-HC	8.77
44[c]	4-$CH_3(CH_2)_3$-C_6H_4	H	H_3C	H_3CO	H_3CO-HC	8.70
45	3-CH_3O-C_6H_4	H	H_3C	H_3CO	H_3CO-HC	8.48
46[a]	4-CH_3CH_2O-C_6H_4	H	H_3C	H_3CO	H_3CO-HC	7.88
47	4-F-C_6H_4	H	H_3C	H_3CO	H_3CO-HC	8.65
48	4-Cl-C_6H_4	H	H_3C	H_3CO	H_3CO-HC	8.51
49[a]	3,4-OCH_2O-C_6H_3	H	H_3C	H3CO	H_3CO-HC	8.38
50	$C_{10}H_7$	H	H_3C	H_3CO	H_3CO-HC	8.88
51[c]	C_6H_5	F_3C	H_3C	H_3CO	H_3CO-HC	9.20
52	3-CH_3-C_6H_4	F_3C	H_3C	H_3CO	H_3CO-HC	8.84
53	4-CH_3-C_6H_4	F_3C	H_3C	H_3CO	H_3CO-HC	8.55
54	3,4-$(CH_3)_2$-C_6H_3	F_3C	H_3C	H_3CO	H_3CO-HC	8.46
55	4-$CH_3(CH_2)_3$-C_6H_4	F_3C	H_3C	H_3CO	H_3CO-HC	8.17
56	3-CH_3O-C_6H_4	F_3C	H_3C	H_3CO	H_3CO-HC	9.35
57	4-F-C_6H_4	F_3C	H_3C	H_3CO	H_3CO-HC	9.08
58	4-Cl-C_6H_4	F_3C	H_3C	H_3CO	H_3CO-HC	9.13
59[c]	4-CH_3CH_2-C_6H_4	F_3C	H_3C	H_3CO	H_3CO-HC	8.79
60[a]	3,4-OCH_2O-C_6H_3	F_3C	H_3C	H_3CO	H_3CO-HC	9.75
61	C_6H_5	H	F_3C	H_3CO	H_3CO-HC	7.00
62[a]	4-CH_3-C_6H_4	H	F_3C	H_3CO	H_3CO-HC	8.28
63	3-CH_3O-C_6H_4	H	F_3C	H_3CO	H_3CO-HC	6.69
64[b]	4-Cl-C_6H_4	H	F_3C	H_3CO	H_3CO-HC	8.17
65	C_6H_5	F_3C	F_3C	H_3CO	H_3CO-HC	7.52
66[c]	4-CH_3-C_6H_4	F_3C	F_3C	H_3CO	H_3CO-HC	6.49
67	4-CH_3CH_2-C_6H_4	F_3C	F_3C	H_3CO	H_3CO-HC	7.04
68	4-CH_3O-C_6H_4	F_3C	F_3C	H_3CO	H_3CO-HC	6.04
69[a]	4-F-C_6H_4	F_3C	F_3C	H_3CO	H_3CO-HC	8.01
70	4-Cl-C_6H_4	F_3C	F_3C	H_3CO	H_3CO-HC	6.67

[a]CoMFA, CoMSIA outlier. [b]HQSAR outlier. [c]Test set. The pI_{50} values were used as dependent variables in the CoMFA and CoMSIA and HQSAR analysis.

method,[15] with a 0.005 kcal/mol energy gradient convergence criterion. Lowest energy conformation was searched by geometry optimization simulated annealing method and minimized conformation energy value was -12.17 kcal/mol.

Molecular alignment. The most important requirement for CoMFA and CoMSIA techniques is that the 3D structures of the molecules should be aligned according to a suitable conformational template. In this study, for most active compounds used as a template molecule, the superimposition of all β-methoxyacrylate analogues was performed with common structure in all the compounds. Figure 1 shows the results of such an alignment.

CoMFA analysis. CoMFA analysis of the 63 methoxyacrylate analogues was carried out on the steric and electrostatic fields with the default values. A three dimensional cubic lattice, with a 1.0, 1.5, 2.0, and 2.5 Å grid spacing, was generated around these molecules. The column filtering 2.0 kcal/mol was set to hasten the analysis and reduce the amount of noise. The steric and electrostatic fields of CoMFA descriptors were calculated separately for each molecule, using an sp^3 carbon atom probe with a Van der Waals radius of 1.52 Å and a charge of +1.0 to generate steric (Lennard-Jones 6-12 potential) and electrostatic (Coulombic potential) fields with a distance dependent dielectric at each lattice point. The SYBYL default energy cut off values of 30.0 kcal/mol were selected for both steric and electrostatic fields. The probe atom was placed at each lattice point and their steric and electrostatic interactions with each atom in the molecule were computed using CoMFA standard scaling.[16,17] Predictive log*P* values were calculated by module program.

CoMSIA analysis. The CoMSIA of the QSAR module of SYBYL was used for the analysis. Similarity indices between a compound and a probe atom were calculated. The common probe atom with charge +1, radius 1.0 Å, and hydrophobicity −1 was placed at the intersections of a regularly spaced lattice.[18,19] The attenuation factor (α) was set at 0.3. To determine the similarity, the mutual distance between probe atom and the atoms of the molecules in the data set was considered. In this study, physicochemical properties, such as steric and electrostatic feature, hydrogen bond donor and acceptors, and hydrophobic field were considered. Eq. (2) used to calculate the similarity index is as follows.

$$A^{q}_{F,k}(j) = -\sum \omega_{probe,k}\omega_{ik}e^{-\alpha r^2_{iq}} \qquad (2)$$

CoMSIA similarity index (A_F) is the similarity index at grid point q, summed over all atoms i of the molecule j under investigation. $\omega_{probe,k}$ is the probe atom with radius 1 Å charge +1, hydrophobicity −1, hydrogen bond donating −1, and hydrogen bond accepting +1. ω_{ik} is the actual value of the physicochemical property k of atom i. The mutual distance between the probe atom at grid point q and atom i of the test molecule is represented by r_{iq}. The default value of 0.3 was used for the attenuation factor (α).[20,21]

Partial least square (PLS) analysis. After eliminating 7 outlier compounds, 53 compounds were used for a training set and 10 compounds were utilized as a test set. Partial least squares (PLS) regression analysis was used in conjugation with the cross-validation option to determine the optimum number of components that, were then used in deriving the final 3D-QSAR model without cross-validation. The cross-validated coefficient, q^2, were calculated using Eq. (3).

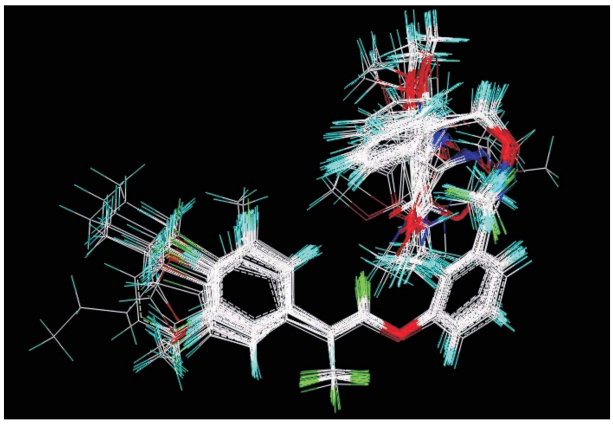

Figure 1. Alignment of the methoxyacrylate analogues.

$$q^2 = 1-|\Sigma(Y_{predicted} - Y_{observed})/\Sigma(Y_{predicted} - Y_{mean})^2| \qquad (3)$$

The number of components that resulted in the highest q^2 and lowest standard error of predictions (SEP) were taken as the optimum. Cross-validation was performed using the leave-one-out (LOO) method in which one compound is removed from the data set and its activity is predicted using the model derived from the rest of the data set. LOO cross-validation was carried out with the number of components set equal to 10 and equal weights were assigned to steric and electrostatic fields, using CoMFA-STD, IND and H-bond scaling options. To speed up the analysis and reduce the noise, a minimum filter value 'σ' of 2.0 kcal/mol was used. Finally, non-cross-validated analysis was performed using the optimal number of previously identified components and was employed to analyze the results of CoMFA and CoMSIA.

HQSAR analysis. An HQSAR study on methoxyacrylate analogues indicated that this technique is able to efficiently correlate molecular structures with biological activity. An HQSAR module of SYBYL was used for the HQSAR study. The quality of the HQSAR model was assessed by statistical methods. The statistical parameter, q^2, was always computed as a measure of the predictive ability of the model by leave-one-out cross-validation, whereas the parameter r^2 was also given to characterize the goodness of fit for the final model. The predictive power of the model was also determined by using a test set. The 53 compounds were used for a training set and 10 compounds were used as a test set. A number of parameters were adjusted to optimize the HQSAR model by various fragment type, length and hologram length. The best model was built using atoms, bonds, and connectivity as

Table 2. Statistical results of CoMFA models

Grid	Field[a]	Statistical values					
		n[b]	F[c] (n1 & n2)	q^2	CN[d]	r^2	S[e]
1.0	S	53	115.642 (10 & 42)	0.544	10	0.965	0.177
1.5	S	53	62.654 (10 & 42)	0.337	10	0.937	0.237
2.0	S	53	79.771 (9 & 43)	0.481	9	0.943	0.222
2.5	S	53	42.672 (5 & 47)	0.525	5	0.819	0.379
1.0	I	53	663.732 (10 & 42)	0.615	10	0.994	0.075
1.5	I	53	243.445 (10 & 42)	0.495	10	0.983	0.123
2.0	I	53	84.372 (5 & 47)	0.462	5	0.900	0.283
2.5	I	53	30.058 (1 & 51)	0.191	1	0.371	0.680
1.0	S+I	53	372.530 (10 & 42)	0.587	10	0.989	0.100
1.5	S+I	53	114.211 (9 & 43)	0.488	9	0.960	0.187
2.0	S+I	53	87.284 (5 & 47)	0.480	5	0.903	0.278
2.5	S+I	53	49.394 (6 & 46)	0.466	6	0.866	0.331
1.0	S+H	53	130.164 (7 & 45)	0.830	7	0.953	0.198
1.5	S+H	53	202.171 (9 & 43)	0.839	9	0.977	0.142
2.0	S+H	53	339.158 (10 & 42)	0.841	10	0.988	0.104
2.5	S+H	53	179.840 (7& 45)	0.833	7	0.965	0.170
1.0	H+I	53	455.115 (10 & 42)	0.832	10	0.991	0.090
1.5	H+I	53	439.235 (10 & 42)	0.836	10	0.991	0.092
2.0	H+I	53	430.606 (10 & 42)	0.858	10	0.990	0.093
2.5	H+I	53	138.696 (6 & 46)	0.791	6	0.948	0.207
1.0	S+I+H	53	358.055 (10 & 42)	0.837	10	0.988	0.102
1.5	S+I+H	53	341.251 (10 & 42)	0.851	10	0.988	0.104
2.0	S+I+H	53	459.780 (10 & 42)	0.858	10	0.991	0.090
2.5	**S+H+I**	**53**	**164.170 (6 & 46)**	**0.822**	**6**	**0.955**	**0.191**

[a]CoMFA with field combinations like standard (S), indicator (I), and H-bond (H) field. [b]Number of compounds. [c]F-test value. [d]Optimum number of components obtained from cross-validated PLS analysis. [e]Standard error of estimate.

fragment type 307 as hologram length and 5-8 as fragment size (Table 7). Activity prediction results by the HQSAR calculation are also summarized in Table 4 and Table 5.

Results and Discussions

CoMFA, CoMSIA, and HQSAR methods were employed for deriving various 3D- and 2D-QSAR models against the total 70 β-methoxyacrylate derivatives (Table 1), keeping *in vitro* activity pI_{50} as a dependent variable. Results of the partial least squares (PLS) analysis are shown in Table 8.

CoMFA analysis. The results of the CoMFA analysis are summarized in Table 8, and for training set and test set, actual and predicted activities are shown in Tables 4 and 5. The statistical results of the CoMFA model in a variety of conditions between field and grid spacing are shown Table 2. The CoMFA was used the observed pI_{50} values of β-methoxyacrylate derivatives as descriptors. Good cross-validated q^2 (0.822) and conventional r^2 (0.955) values were proposed with optimized components of 6, the best model fields were used by Standard, Indicator, and H-bond field at 2.5 grid spacing. The quality of the CoMFA models is represented in Figure 3, which shows plots of observed

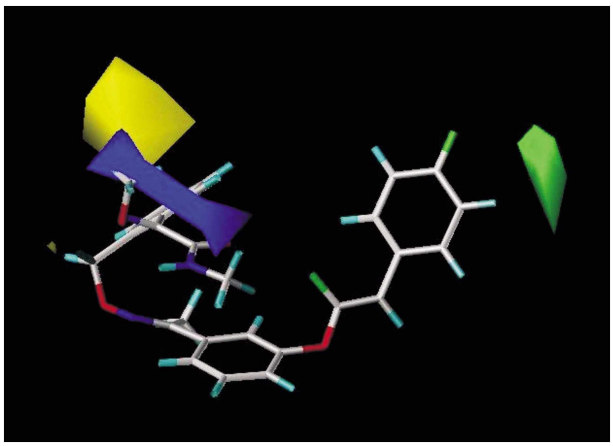

Figure 2. CoMFA contour map of Methoxyacrylate analogues. Steric contour plots. Green contours indicate regions where bulky groups increase activity.

biological activity versus activity predicted from the best CoMFA model at 2.5 grid spacing. The contributions of steric and electrostatic fields were 0.762 and 0.238, respectively. The CoMFA steric and electrostatic fields for the analysis are presented as contour maps in Figure 2. In general, color polyhedrals surrounded lattice points where the QSAR strongly associated changes in compound field values with changes in biological potency. A green polyhedral surrounded regions where more bulk is favorable for increasing potency, whereas a yellow polyhedral surrounded regions where less bulk is good. Red and blue contours show regions of desirable negative and positive electrostatic interactions, respectively. Electrostatic contours indicate the location of the electropositive character on R_4 position in blue color, indicating an enhancement in fungicidal activity, and so a blue contour near the R_5 position explains the need of an electron-unrich (electropositive) group to show potent fungicidal activity. We could conclude that the fungicidal activity was increased by a steric bulky group at R_1 position, and regions of the R_4 and R_5 positions were located in the

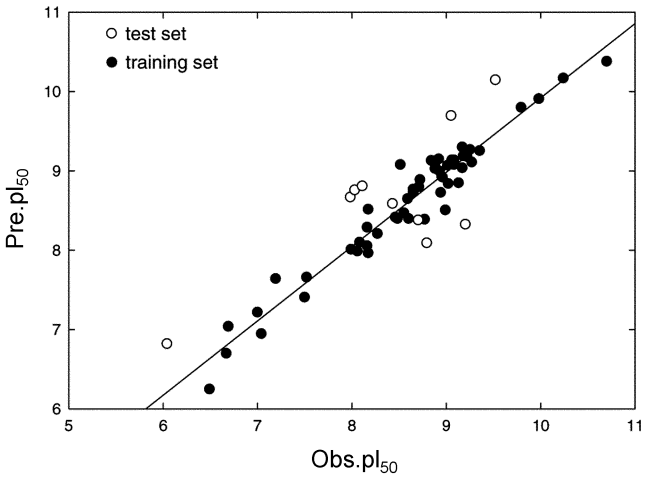

Figure 3. Relationship between observed values (obs.) and prediction values (pred.) by CoMFA methodology for the fungicidal activities of *Magnaporthe grisea* (Rice Blast Disease).

Table 3. Statistical results of CoMSIA models

Grid	Field[a]	Statistical values					
		n[b]	F[c] (n1 & n2)	q^2	CN[d]	r^2	S[e]
1.0	S	53	16.881 (5 & 47)	0.206	5	0.642	0.534
1.5	S	53	17.407 (5 & 47)	0.216	5	0.649	0.529
2.0	S	53	21.893 (5 & 47)	0.239	5	0.700	0.489
2.5	S	53	22.283 (1 & 51)	0.176	1	0.304	0.715
1.0	E	53	0.150 (1 & 51)	0	1	0.003	0.856
1.5	E	53	0.145 (1 & 51)	0	1	0.003	0.856
2.0	E	53	0.145 (1 & 51)	0	1	0.003	0.856
2.5	E	53	0.145 (1 & 51)	0	1	0.003	0.856
1.0	H	53	50.749 (8 & 44)	0.757	8	0.902	0.289
1.5	H	53	55.665 (7 & 45)	0.750	7	0.896	0.294
2.0	H	53	68.492 (7 & 45)	0.772	7	0.914	0.267
2.5	H	53	49.230 (9 & 43)	0.786	9	0.912	0.278
1.0	H-D	53	3.608 (6 & 46)	0.126	6	0.320	0.744
1.5	H-D	53	4.419 (5 & 47)	0.230	5	0.320	0.736
2.0	H-D	53	18.670 (1 & 51)	0.006	1	0.268	0.733
2.5	H-D	53	18.395 (1 & 51)	0.006	1	0.265	0.735
1.0	H-A	53	30.399 (2 & 50)	0.186	2	0.549	0.581
1.5	H-A	53	21.217 (2 & 50)	0.174	2	0.459	0.637
2.0	H-A	53	15.466 (2 & 50)	0.100	2	0.382	0.680
2.5	H-A	53	15.573 (2 & 50)	0.124	2	0.384	0.679
1.0	S+H	53	58.667 (9 & 43)	0.746	9	0.925	0.256
1.5	S+H	53	58.178 (9 & 43)	0.742	9	0.924	0.257
2.0	**S+H**	**53**	**84. 361 (6 & 46)**	**0.763**	**6**	**0.917**	**0.260**
2.5	S+H	53	69.635 (6 & 46)	0.772	6	0.901	0.284

[a]CoMSIA with field combinations like steric(S), electrostatic(E), hydrophobic (H), H-bond donor(D), and H-bond acceptor (A) field. [b]Number of compounds. [c]F-test value. [d]Optimum number of components obtained from cross-validated PLS analysis. [e]Standard error of estimate.

steric disfavorable and positive charge groups. The CoMFA analysis on the test set composed of another 10 β-methoxyacrylate derivatives was reported in Table 5. Most of the test set compounds showed good agreement between actual and predicted values, with 0.257 of average value of the deviation

CoMSIA analysis. CoMSIA is believed to be less affected by changes in molecular alignment, and it provides more smooth and interpretable contour maps. The results of the CoMSIA analysis are summarized in Table 8, and actual and predicted activities of training and test set are shown in Table 4 and Table 5. The statistical results of the CoMSIA model in a variety of conditions between fields and grid spacing are shown in Table 3. CoMSIA used the observed pI_{50} values of β-methoxyacrylate derivatives as descriptors. Good cross-validated q^2 (0.763) and conventional r^2 (0.917) values were proposed, with an optimized component of 6; the best model fields were used by hydrophobic, and steric at 2.0 grid spacing. The quality of the CoMSIA models is represented in Figure 5, which shows plots of observed biological activity versus activity predicted from the best CoMSIA model at 2.0 grid spacing. The contributions of hydrophobic and steric fields were 0.749 and 0.251,

Table 4. Observed fungicidal activities (pI_{50}) and prediction values by CoMFA, CoMSIA and HQSAR methodology

Entry.	Obs.	CoMFA		CoMSIA		HQSAR	
		Pre.	Dev.	Pre.	Dev.	Pre.	Dev.
2	8.72	8.59	0.13	8.75	-0.03	8.95	-0.23
3	8.95	8.87	0.08	8.85	0.1	9.14	-0.19
5	7.99	8.05	-0.06	8.47	-0.48	8.37	-0.38
6	8.27	8.31	-0.04	8.23	0.04	7.98	0.29
7	8.16	8.21	-0.05	8.21	-0.05	7.86	0.3
9	8.6	8.49	0.11	8.32	-0.28	8.57	0.03
10	8.16	8.61	-0.45	8.37	-0.21	8.49	-0.33
11	9.25	9.03	0.22	9.26	-0.01	9.56	-0.31
12	9.98	9.91	0.07	10.04	-0.06	9.77	0.21
13[a]	9.89	–	–	–	–	9.61	0.28
14	8.65	8.75	-0.1	8.46	0.19	8.66	-0.01
15[b]	10.7	9.61	1.09	10.32	0.38	–	–
16	8.96	9	-0.04	8.87	0.09	9	-0.04
17	8.88	9.14	-0.26	9	-0.12	9.06	-0.18
18[b]	8.94	8.92	0.02	8.94	0	–	–
19	9.06	9.01	0.05	8.86	0.2	9.08	-0.02
20	8.71	8.81	-0.1	8.8	-0.09	8.52	0.19
22	8.08	8.02	0.06	8.41	-0.33	8.32	-0.24
23	9.08	9.05	0.03	8.5	0.58	9.2	-0.12
24	8.59	8.56	0.03	8.89	-0.3	8.23	0.36
25	9.27	9.04	0.23	8.9	0.37	9.35	-0.08
26	9.17	9	0.17	8.86	0.31	8.83	0.34
27	8.93	9.03	-0.1	8.95	0.02	9.35	-0.42
28[b]	9.18	8.67	0.51	9 16	0.02	–	–
29	9.01	9.05	-0.04	8.86	0.15	8.79	0.22
30	9.79	9.68	0.11	9.5	0.29	9.8	-0.01
31	8.92	9.25	-0.33	8.89	0.03	9.22	-0.3
33	10.24	10.03	0.21	10.58	-0.34	10.15	0.09
35	7.5	7.23	0.27	7.55	-0.05	7.32	0.18
36	7.19	7.49	0.2	7.18	0.51	7.38	-0.19
37[b]	8.06	6.99	1.07	7.9	0.16	–	–
38	9.22	9.2	-0.13	9.09	-0.02	8.79	0.43
39	9.17	9.43	0	9.22	0.21	8.99	0.18
40	8.99	8.65	0.09	8.85	-0.11	8.71	0.28
41	9.02	8.94	0.08	8.46	0.56	8.97	0.05
43	8.77	8.55	0.22	8.18	0.59	8.84	-0.07
45	8.48	8.58	-0.1	8.55	-0.07	8.39	0.09
46[a]	7.88	–	–	–	–	7.89	-0.01
47	8.65	8.84	-0.19	8.94	-0.29	8.94	-0.29
48	8.51	9.08	-0.57	9.06	-0.55	8.92	-0.41
49[a]	8.38	–	–	–	–	8.48	-0.1
50	8.88	9.07	-0.19	8.41	0.47	8.85	0.03
52	8.84	9.15	-0.31	9.23	-0.39	9.09	-0.25
53	8.55	8.5	0.05	9.03	-0.48	8.44	0.11
54	8.46	8.72	-0.26	8.47	-0.01	8.54	-0.08
55	8.17	8.32	-0.15	8.72	0.55	8.35	-0.18
56	9.35	9.05	0.3	9.2	0.15	9.23	0.12
57	9.08	9.01	0.07	9.14	-0.06	9.37	-0.29
58	9.13	8.82	0.31	9.12	0.01	8.86	0.27
60[a]	9.75	–	–	–	–	9.37	0.38
61	7	7.13	-0.13	7.14	-0.14	7.1	-0.1
63	6.69	7.03	-0.34	7.2	-0.51	6.71	-0.02
64[b]	8.17	7.31	0.86	7.74	0.43	–	–
65	7.52	7.46	0.06	7.76	-0.24	7.34	0.18
67	7.04	6.73	0.31	6.77	0.27	6.87	0.17
68	6.04	6.43	-0.39	7.04	-1	6.57	-0.53
69[a]	8.01	–	–	–	–	7.69	0.32
70	6.67	6.81	-0.14	7.11	-0.44	7.17	-0.5

[a]CoMFA, CoMSIA outlier; [b]HQSAR outlier

Table 5. Predicted value of the test set compounds in CoMFA, CoMSIA and HQSAR

Entry.	Obs.	CoMFA		CoMSIA		HQSAR	
		Pre.	Dev.	Pre.	Dev.	Pre.	Dev.
1	7.98	8.47	-0.49	8.53	-0.55	8.69	-0.71
4	8.03	8.14	-0.11	8.03	0.00	8.60	-0.57
8	8.43	8.53	-0.10	8.72	-0.29	8.91	-0.48
21	8.11	8.41	-0.30	8.45	-0.34	7.84	0.27
32	9.05	9.24	-0.19	9.23	-0.18	9.33	-0.28
34	9.52	9.62	-0.10	9.55	-0.03	9.72	-0.20
44	8.70	8.73	-0.03	8.42	0.28	8.63	0.07
51	9.20	8.71	0.49	8.52	0.68	9.03	0.17
59	8.79	8.29	0.50	8.23	0.56	8.56	0.23
66	6.49	6.23	0.26	6.71	-0.22	6.76	-0.27
Average			0.257		0.313		0.325

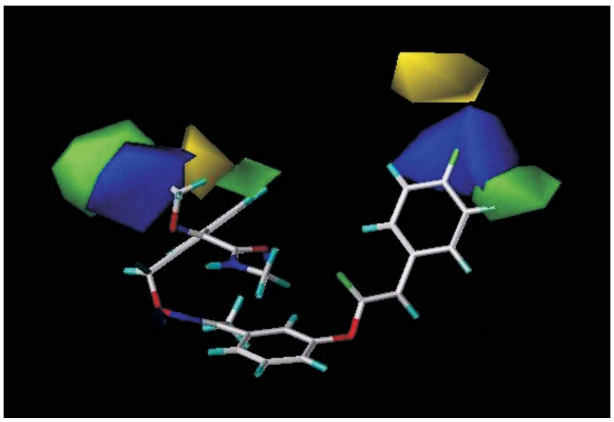

Figure 4. CoMSIA contour map of Methoxyacrylate analogues. Steric contour plots, green contours indicate regions where bulky groups increase activity. Hydrophobic whereas blue contours indicate regions where hydrophobic groups decrease activity.

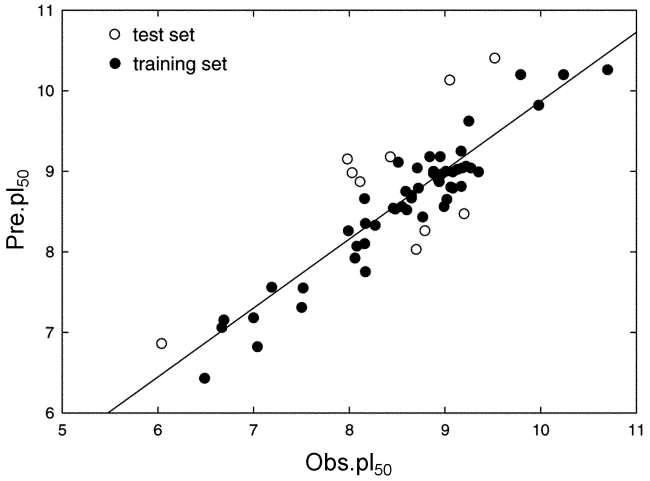

Figure 5. Relationship between observed values (obs.) and prediction values (pred.) by CoMSIA methodology for the fungicidal activities of *Magnaporthe grisea*(Rice Blast Disease).

respectively. The CoMSIA hydrophobic and steric fields for the analysis are presented as contour maps in Figure 4. In general, the color polyhedral surrounded lattice points where the QSAR strongly associated changes in compound field values with changes in biological potency. A blue polyhedral surrounded regions where more hydrophobicity is favorable for increasing potency, whereas a red polyhedral surrounded regions where less hydrophobicity is good. Green and yellow contours show regions of desirable steric interactions. We could conclude that the fungicidal activity was increased by creation of R_5 position is hydrophobic favorable and R_1 position is hydrophobic and steric favorable.

Apparently the properties of the whole group of β-methoxyacrylate analogues are not sufficiently represented by the few compounds available, although they seem to fit into the overall model.

HQSAR analysis. Results of HQSAR calculations are summarized in Tables 8. We multiply performance for the influence of the fragment distinction and the fragment size. The results of the influence of fragment size are summarized in Table 6. This represents a moderate size, which may be expected to give acceptable results; the best fragment size (q^2=0.82, with a standard error of 0.39; r^2, final: 0.92; standard error, final: 0.26) was obtained with a size of 5-8. Table 7 shows HQSAR analysis for various fragment distinctions on the key statistical parameters, using default fragment size. Selection of the best model for fragment distinction was based on atom, bond and connectivity information.

The results of HQSAR analyses for various hologram lengths are shown in Figure 6. The cross validated parameter (q^2) showed a significant dependence on the hologram

Table 6. HQSAR analysis for the influence of various fragment sizes on the key statistical parameters using the best fragment distinction (atoms, bonds and connectivity)

Fragment size	Statistical parameters				
	q^2	SEcv	r^2	SE	NC
2-5	0.732	0.488	0.854	0.359	9
3-6	0.750	0.476	0.883	0.326	10
4-7	0.806	0.419	0.922	0.266	10
5-8	**0.820**	**0.391**	**0.919**	**0.262**	**7**
6-9	0.814	0.397	0.920	0.260	7
7-10	0.805	0.411	0.923	0.258	8

Table 7. HQSAR analysis for the various fragment distinction on the key statistical parameters using fragment size default (**5-8**)

Fragment distinction	Satistical parameters				
	q^2	SEcv	r^2	SE	NC
Atom/bond[a]	0.800	0.411	0.912	0.273	7
Connectivity (Con)	**0.820**	**0.391**	**0.919**	**0.262**	**7**
Hydrogen (H)	0.794	0.427	0.919	0.268	9
Con-H	0.787	0.439	0.917	0.274	10

[a]In all case, the *atoms* and *bonds* flags are turned on.

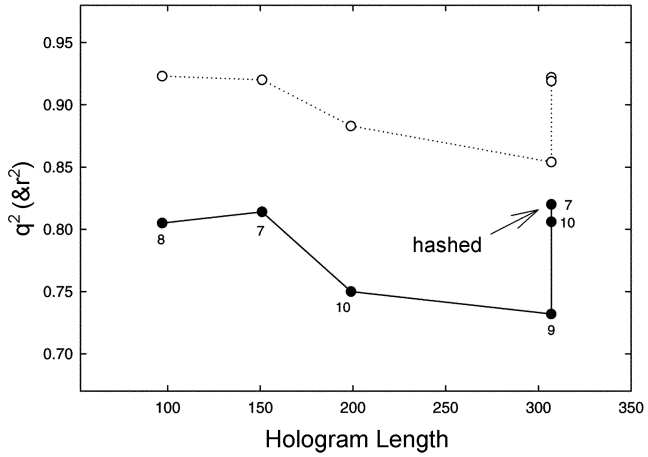

Figure 6. Variation of q^2 (●) and r^2 (○) as a function of hologram length (bin) in HQSAR models.

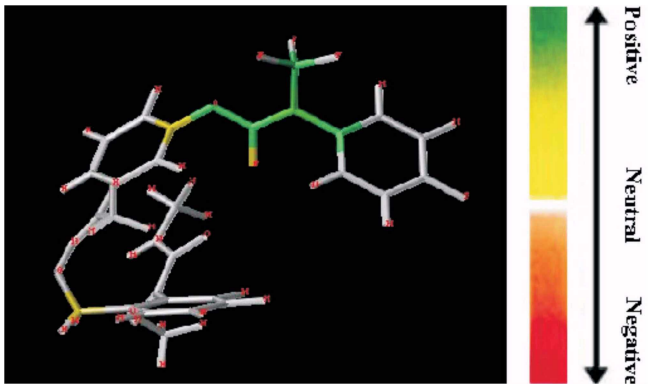

Figure 7. Contribution map of *Magnaporthe grisea* (Rice Blast Disease) using HQSAR methodology.

length; the best value was obtained with a length of 307, with seven components.

Figure 7 shows that the contribution maps on *Magnaporthe grisea* (Rice Blast Disease), using HQSAR methodology. In the contour map, the high potency active site is represented by green. Based on these results, the fluorostyrene site contributed to fungicidal activities. The results of the correlation of the molecular hologram descriptor and biological activity gave a good r^2 value (0.919), a cross-validated q^2 value (0.820) and included an optimum number of seven components for minimizing model complexity.

The HQSAR actual versus predicted activity for the training set are shown in Table 4 and plotted in Figure 8. Measured biological data of the test set together with predicted values by the HQSAR calculation are summarized in Table 5. The plot of predicted vs. measured values for the test set is shown in Figure 8. It gave good predictive power as shown in Figure 8.

Prediction for the compounds in the test set. The predicted model was used to predict the inhibitory activities of the compounds in the test set. Predicted and actual pI_{50} values for CoMFA, CoMSIA and HQSAR for training and test set are plotted in Figures 3, 5 and 8. The comparison of

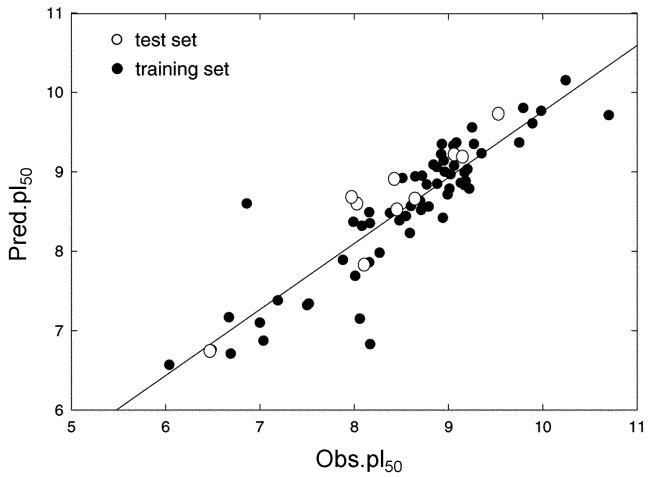

Figure 8. Relationship between observed values (obs.) and prediction values (pred.) by HQSAR methodology for the fungicidal activities of *Magnaporthe grisea* (Rice Blast Disease).

Table 8. Models of CoMFA, CoMSIA and HQSAR methodology

Statistical & Fraction	CoMFA	CoMSIA	HQSAR
Number of data set compounds	53	53	53
F	164.170	84.361	–
r^2	0.955	0.917	0.919
Predictive correlation coefficient (q^2)	0.822	0.763	0.820
Std error of estimate	0.191	0.260	0.262
Grid spacing (Å)	2.5	2.0	–
Number of component	6	6	7
Standard; Steric	0.137	–	–
Electrostatic	0.186	–	–
Indicator; Steric	0.193	–	–
Electrostatic	0	–	–
H-bond Steric	0.432	–	–
Electrostatic	0.052	–	–
Steric	–	0.251	
Electrostatic	–	–	
Hydrophobic	–	0.749	–
H-bond donor	–	–	–
Molecular Fragment	–	–	5-8
Best length	–	–	151
H-Atom (On or Off)	–	–	off

the observed and predicted biological activities of the test set is given in Table 5, which shows clearly the usefulness of the model for the prediction of the activities on the compounds that are not included in the training set. The derivation values (Table 5) indicate that CoMFA, CoMSIA, and HQSAR models can accurately predict the activities of all compounds in the test set. Based on the PLS statistics of CoMFA and CoMSIA 3D-models, CoMFA is clearly better than CoMSIA. Predictability of CoMFA and HQSAR also shows that CoMFA is better than HQSAR. The CoMFA model gave the best cross-validated q^2 value (0.822), CoMSIA and HQSAR show good predictability for cross-validated q^2 values, 0.763 and 0.820, respectively.

Conclusion

We have established predictive CoMFA and CoMSIA 3D-QSAR models and HQSAR 2D-QSAR model for β-methoxyacrylate analogues as inhibitory activity against *Magnaporthe grisea* (Rice Blast Disease). In CoMFA on the β-methoxyacrylates, cross-validated q^2 is 0.822 and r^2 is 0.955; the contributions of steric and electrostatic fields are 0.762 and 0.238, respectively. In CoMSIA, cross-validated q^2 is 0.763 and conventional r^2 is 0.917. In HQSAR, cross-validated q^2 is 0.820 and conventional r^2 is 0.919. Predictions resulting from CoMFA, CoMSIA and HQSAR models on 10 compounds in the test set are in good agreement with experimentally determined values. The results provide the tools for predicting the biological activity of related compounds and for guiding the design of new β-methoxyacrylate having more potent inhibitory activity.

Acknowledgement. This work was supported by the Ministry of Science and Technology (MOST) and a grant (No. R11-2002-100-03002-2) from the ERC program of the Korea Science & Engineering Foundation.

References and Notes

1. Konradt, M.; Kappes, E. M.; Hiemer, M.; Peterson, H. H. *Gesunde Pflanzen* **1996**, *48*(4), 126.
2. Dave, W. B.; John, M. C.; Jeremy, R. G. *Pest Manag Sci.* **2002**, *58*, 649.
3. Tamura, H.; Mizutani, A. *Nippon Noyaku Gakkaishi* **1999**, *24*(2), 189.
4. Wittman, M. D.; Kallmerten, J. *J. Org. Chem.* **1987**, *52*(19), 4303.
5. Martin, B. J.; Clough, J. M.; Pattenden, G.; Waldron, I. R. *Tetrahedron Letters* **1993**, *34*(32), 5151.
6. Crammer, R. D., III; Patterson, D. E.; Bunce, J. D. *J. Am. Chem. Soc.* **1988**, *110*, 5959.
7. Gokhale, V. M.; Kulkarni, V. M. *J. Med. Chem.* **1999**, *42*, 5348.
8. Klebe, G.; Abraham, U.; Mietzner, T. *J. Med. Chem.* **1994**, *37*, 4130.
9. Borosy, A. P.; Keseru, K.; Penzes, I.; Matyus, P. *J. Molecular Structure (Theochem)* **2000**, *503*, 113.
10. Rambard, M.; Bakasse, H.; Duguay, G.; Villieras, J. *Synthesis* **1988**, 564.
11. Yamada, K.; Kato, M.; Hirata, Y. *Tetrahedron Lett.* **1973**, *14*, 2745.
12. Herkes, F. E.; Burton, D. J. *J. Org. Chem.* **1967**, *32*, 1311.
13. Nemeth, G.; Rakoczya, E.; Simiga, G. *J. Fluorine Chem.* **1996**, *76*, 91.
14. *SYBYL 6.9*, Tripos Inc.; USA, 0000.
15. Gasteteiger, J.; Marsili, M. *Tetrahedron* **1980**, *36*, 3219.
16. Purushottamachar, P.; Kulkarni, V. M. *Biooragnic & Medicinal Chemistry* **2003**, *11*, 3487.
17. Roh, E. J.; Kim, D.; Choi, J. Y.; Lee, B. S.; Lee, C. O.; Song, C. E. *Bioorganic & Medicinal Chemistry* **2002**, *10*, 3135.
18. Hou, T.; Li, Y.; Liao, N.; Xu, X. *J. Mol. Model* **2000**, *6*, 438.
19. Islam, M. N.; Song, Y.; Iskander, M. N. *J. Molecular Graphics and Modeling* **2003**, *21*, 263.
20. Choo, H. P.; Choi, S.; Ryu, C. K.; Kim, H. J.; Lee, I. Y.; Pae, A. N.; Koh, H. Y. *Biooragnic & Medicinal Chemistry* **2003**, *11*, 2019.
21. Xu, M.; Zhang, A.; Han, S.; Wang, L. *Chemosphere* **2002**, *48*, 707.
22. Kim, B. T.; Park, N. K.; Kim, J. C.; Choi, K. J.; Park, C. S. U.S. Pat. 6552080 **2003**/04/22 Fungicidal compounds having a fluorovinyl or fluoropropenyl-oxyphenyloxime moiety and process for the preparation thereof.